

ORIGIN AND EVOLUTION OF ICES IN STAR-FORMING REGIONS

A VLT-ISAAC 3–5 μm SPECTROSCOPIC SURVEY

THE VLT HAS OPENED UP THE POSSIBILITY TO PERFORM SPECTROSCOPIC SURVEYS OF LARGE NUMBERS OF YOUNG LOW-MASS STARS WHICH ARE STILL DEEPLY EMBEDDED IN THEIR PARENTAL CLOUDS. OUR INFRARED SPECTRA SHOW A RICH VARIETY OF FEATURES DUE TO ICES AND GAS-PHASE MOLECULES, EACH OF WHICH TRACE DIFFERENT ASPECTS OF THE PHYSICAL AND CHEMICAL STATE OF THE OBJECTS. HIGHLIGHTS INCLUDE FUNDAMENTAL NEW INSIGHT INTO THE STRUCTURE OF INTERSTELLAR ICES; THE FIRST DETECTION OF SOLID METHANOL IN LOW-MASS PROTOSTARS, A KEY INGREDIENT FOR BUILDING MORE COMPLEX ORGANIC MOLECULES; DIRECT EVIDENCE FOR SIGNIFICANT FREEZE-OUT IN EDGE-ON CIRCUMSTELLAR DISKS; AND SENSITIVE LIMITS ON MINOR ICE COMPONENTS SUCH AS AMMONIA AND DEUTERATED WATER.

E. F. VAN DISHOECK¹,
 E. DARTOIS²,
 K. M. PONTOPPIDAN¹,
 W. F. THI^{1,3},
 L. D'HENDECOURT²,
 A. C. A. BOOGERT⁴,
 H. J. FRASER⁵,
 W. A. SCHUTTE⁵,
 A. G. G. M. TIELENS⁶

¹Leiden Observatory,
 The Netherlands;

²IAS, Paris, France;

³Sterrenkundig Instituut,
 Amsterdam, The

Netherlands; ⁴Caltech,

Pasadena, USA; ⁵Sackler

Laboratory, Leiden

Observatory, The

Netherlands; ⁶Kapteyn

Observatory/SRON,

Groningen, The Netherlands

Figure 1: Schematic illustration of infrared absorption line observations of gas and dust toward embedded or background sources. The infrared continuum (red color) is provided by the hot dust at 300–1000 K very close to the YSO (region not drawn to scale) against which cooler material (blue color) along the line-of-sight is seen in absorption.

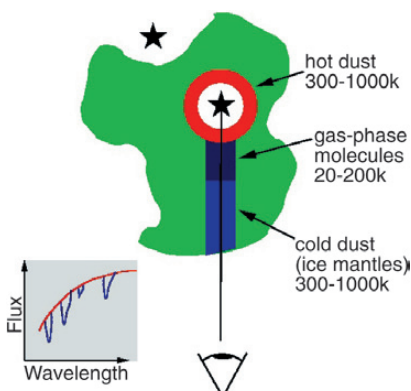
WHEN STARS FORM DEEP inside dense molecular clouds, the surrounding gas and dust become part of the infalling envelope feeding the central object. In the earliest stages, the nascent protostars are extinguished by hundreds to thousands of magnitudes, so that only the circumstellar gas and dust can give a glimpse of what is happening inside. A study of their evolution is therefore key to understanding solar origins. Part of this gas and dust ends up in the rotating discs surrounding the young stars, and forms the basic material from which icy planetesimals, and ultimately planets, are formed. A spectroscopic survey of a set of embedded young low-mass stars, such as that performed by our team with VLT-ISAAC, thus also provides quantitative information on the chemical building blocks available during planet formation.

Due to the high dust obscuration, star birth is best studied at long wavelengths. Most young stellar objects (YSO's) have been found through IRAS and ground-based infrared surveys, and have the peak

of their spectral energy distribution at far-infrared wavelengths. The spectra of the coldest protostellar objects (ages of $\sim 10^4$ yr since collapse began) peak around 100 μm and such sources are best studied with submillimeter telescopes. Once the dense envelopes start to dissipate due to the effects of outflows, the objects become detectable at infrared wavelengths, around ages of $\sim 10^5$ yr. Both regions have their advantages for studying circumstellar material. In the submillimeter, thermal continuum emission from cold ($T_{\text{dust}} \approx 10 - 50$ K) dust is seen, as well as spectral lines from a plethora of gas-phase molecules. Owing to the heterodyne technique, the spectral resolving power of these data is intrinsically extremely high, $R = \lambda/\Delta\lambda > 10^6$ or $\Delta V < 0.1$ km/s, so that the detailed kinematics of the region can be studied. Until the advent of large millimeter interferometers such as ALMA, however, the spatial resolution of these data remains poor.

Mid-infrared spectroscopy has the advantage that the composition of both the gas and the dust can be studied. Solid-state material has characteristic broad vibrational transitions in the infrared, but no strong bands at millimeter wavelengths. In this case, the features are often seen in absorption against the hot ($T_{\text{dust}} > 300$ K) dust in the immediate surroundings of the young star (Fig. 1). At $R > 2000$, the gas-phase lines – which are intrinsically much narrower – also become visible, albeit only for the most abundant molecules.

The earliest mid-infrared spectra of YSO's were obtained in the 1970's and 1980's, mostly with the Kuiper Airborne Observatory and UKIRT (see van Dishoeck & Tielens 2001 for a historical



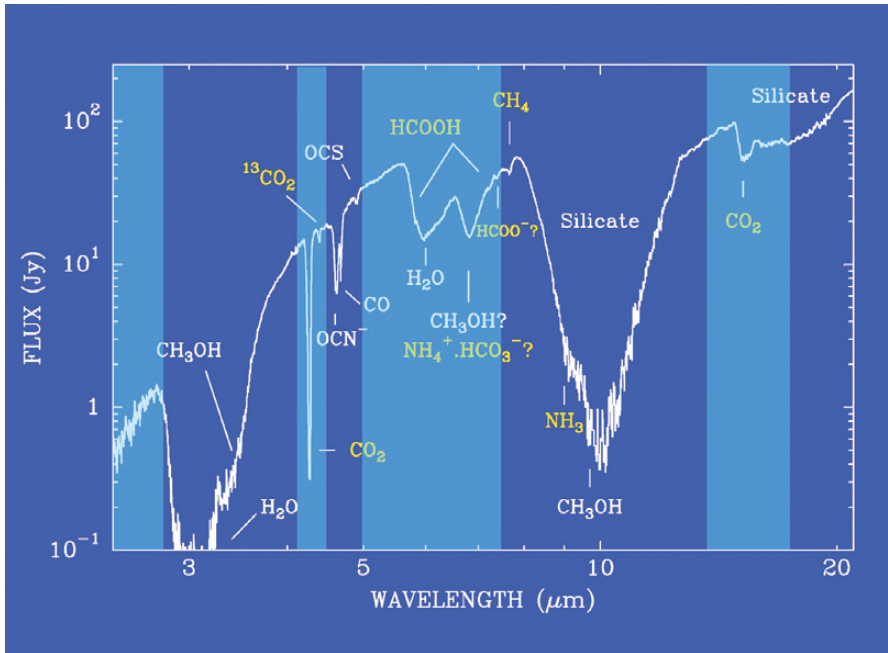


Figure 2: ISO-SWS spectrum of the deeply embedded massive YSO W 33A (Gibb et al. 2000, *ApJ* 536, 347). Various absorption features due to silicate grain cores and icy mantles are indicated. Regions which cannot be observed from the ground are shaded. Our large programme covered the 2.85–4.1 μm (L-band) and 4.5–5.1 μm (M-band) windows.

review). At the low spectral resolution of those data, only solid-state bands were detected, but the spectra of some massive protostars already revealed a surprising wealth of features. These included not only the anticipated bands of the silicate grain cores at 9.7 and 18 μm due to the Si-O stretching and bending modes, but also other broad features. Thanks to detailed interaction with laboratory astrophysicists (including some of the authors at that time!), these could soon be ascribed to ice mantles, in particular H₂O ice and CO ice.

The big step forward came in 1995 with the launch of the Infrared Space Observatory (ISO). The Short Wavelength Spectrometer (SWS) on ISO provided the first opportunity to obtain mid-infrared spectra over the entire 2.5–20 μm range unhindered by the Earth's atmosphere. High quality data were obtained for about a dozen YSO's, revealing several new features and allowing a much more reliable identification of other species (Fig. 2). Several important ingredients of ices, such as CO₂, CH₄ and CH₃OH, were firmly established with abundances ranging from < 1% up to 30% of that of H₂O ice. However, the ISO-SWS only had the sensitivity to observe sources forming massive O or B stars with luminosities >10⁴ L_⊙.

The advent of 8–10 m class telescopes equipped with infrared spectrometers with large-format arrays has opened up the possibility to study low-mass protostars with luminosities comparable to that

of our Sun. Although hampered by the atmosphere, the sensitivity of these facilities is such that a large sample of objects can be surveyed in a relatively short time. Accordingly, we proposed in 1999 a large VLT-ISAAC programme to perform a spectroscopic 3–5 μm survey of YSO's in the southern hemisphere. The main goals were to: (i) obtain an inventory of the major and minor ice components in a large set of low- and intermediate-mass YSO's

(< 10³ L_⊙) and some circumstellar discs, and study evolutionary and environmental effects by comparison with high-mass sources and comets; (ii) use gaseous and solid-state features to probe the physical conditions and thermal history of the protostellar environment; and (iii) constrain the basic ice structure through comparison with experimental data obtained in our laboratories in Leiden and Paris.

OUR VLT-ISAAC LARGE PROGRAMME

In mid-1999, we were allotted 14 nights to survey 30–50 southern YSO's, but due to a long string of technical difficulties, our first observing run did not take place until January 2001. At that time, ISAAC had been upgraded with a 1024×1024 Aladdin array improving the efficiency of our observations, so that the programme could be finished in May 2002. Because our team was the first to use the long-wavelength spectroscopic mode of ISAAC, we had to build up much of the experience on how to use the instrument ourselves. Also, there was no pipeline data reduction at the time, so we had to develop codes for quick-look at the telescope and more detailed off-line data reduction. Several observing runs in visitor mode were crucial to gain familiarity with the instrument and devise an optimal observing strategy.

The L-band window from 2.85–4.1 μm was surveyed in the low spectral resolution mode (1 spectral setting), whereas the M-band window from 4.5–5.1 μm was

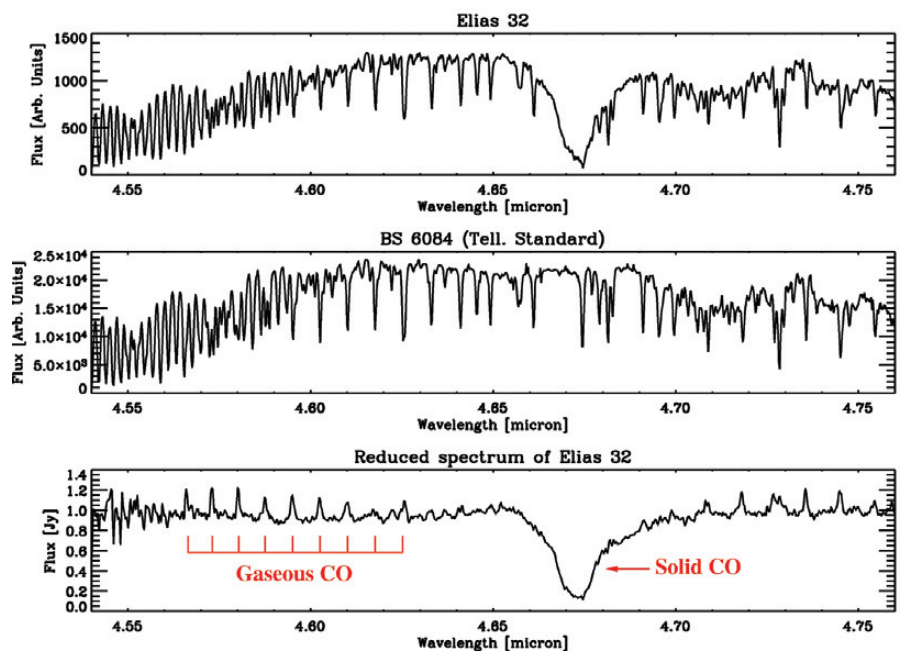
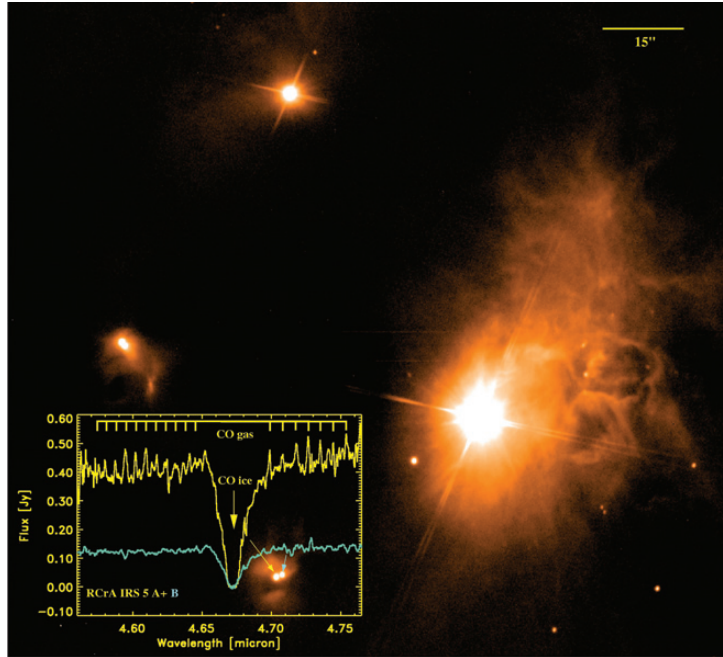


Figure 3: Raw spectrum of the source Elias 32 (top) and a standard star (middle), illustrating the forest of telluric features at M-band. The bottom spectrum shows the source spectrum with the atmospheric lines divided out. These features are best removed by observing at the highest spectral resolution.

Figure 4: VLT-ISAAC K' image of the R CrA cluster, with several of our targets indicated. The spectra of the 5A and 5B binary (few hundred AU separation) are shown, illustrating similarities and differences on small scales.



observed in medium resolution mode (2 spectral settings required to cover the entire band; often only a single setting from 4.55–4.75 μm was taken). After the first observing run, it became clear that the S/N was dominated by our ability to remove atmospheric features (Fig. 3) and that the best strategy was to observe at the highest spectral resolution, i.e., smallest slit width. Accordingly, all subsequent spectra were obtained with the 0.3'' slit, resulting in $R \approx 1200$ at L-band and $R \approx 10,000$ at M-band. Slit losses due to seeing were found to be minimal, even when the optical seeing was close to 1''. Standard spectra of bright unreddened early-type stars were obtained immediately before or after each source, as close as possible in airmass (< 0.1 difference).

The sources were chosen from infrared surveys of southern star-forming clouds, including Ophiuchus, Chamaeleon, Corona Australis, Vela, Orion, and Serpens. Although 2.5 of the 14 nights were lost due to bad weather, 60 sources at L-band and 45 at M-band were observed. We were able to survey more objects than envisaged in the original proposal because several new sources were picked up in the acquisition images at 2–15'' distance from the main target. By rotating the slit, the spectrum of the weaker, second component could be obtained simultaneously and was often of good enough quality for analysis. This also gives interesting information on the small-scale structure of the clouds, on scales down to a few hundred AU (Fig. 4). Typical integration times were 20 minutes on source, with the

longest integration being 2 hr. This gave $S/N > 30$ on sources with $L \sim 9$ mag (0.07 Jy) and $M \sim 8$ mag (0.1 Jy).

Since the detailed line shapes are crucial for our analysis, extensive checks were done to explore the reproducibility. Spectra obtained on different nights and with different standard stars were compared, as were low- versus medium-resolution spectra. More revealing is the comparison with spectra obtained at other facilities, in particular ISO, UKIRT and Keck. Figure 5 shows the spectra of a northern YSO, L1489 in Taurus, obtained with both VLT-ISAAC and Keck-NIRSPEC. In spite of the large airmass

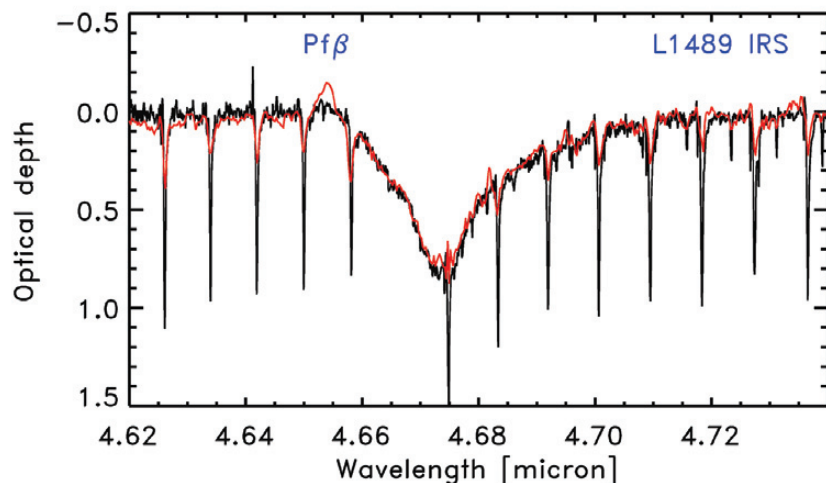


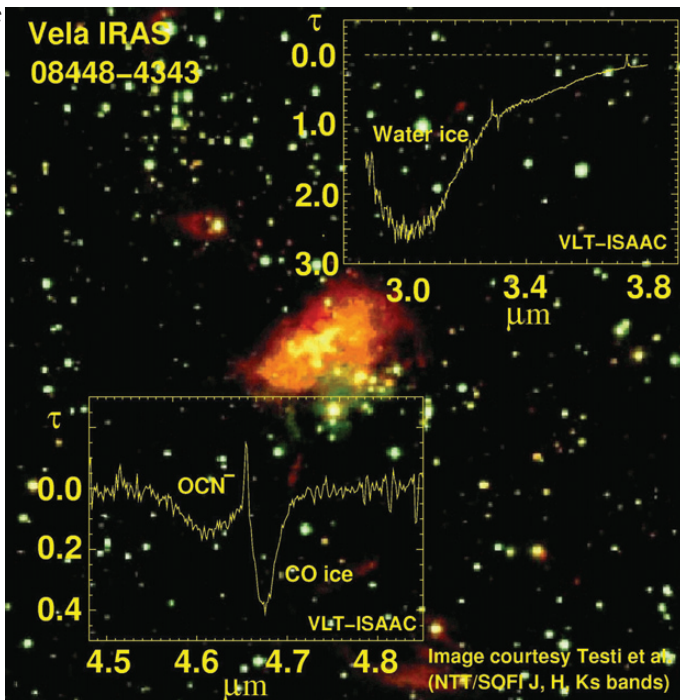
Figure 5: Comparison of the VLT-ISAAC (red) and Keck-NIRSPEC (black, Boogert et al. 2002) spectra of L1489 in Taurus. Note the excellent agreement in the shape of the solid CO feature. The gas-phase absorptions are deeper in the Keck spectrum due to its higher resolving power ($R \approx 25,000$ vs 10,000), which also aids in removing the telluric features.

from Chile, the agreement between the two spectra is excellent and the shape of the solid CO band is well reproduced, confirming Paranal as a good mid-infrared site in spite of its lower altitude than Mauna Kea. As expected, the gas-phase CO absorptions are deeper in the higher resolution $R \approx 25,000$ Keck spectra.

As Fig. 2 shows, the L- and M-band windows include only a limited number of features and are dominated by the H_2O ice at 3 μm and CO gas and ice bands at 4.67 μm , respectively (see also Fig. 6). At $R > 2000$, CO ice can be readily distinguished from CO gas as it consists of a single broad vibrational band: because the molecule is trapped in the ice matrix, it cannot freely rotate. In contrast, CO gas shows a number of narrow lines due to the simultaneous vibration and rotation of the molecule. H_2O and CO ice were detected in more than 90% of our sources. The abundances of H_2O ice are typically 10^{-5} – 10^{-4} with respect to H_2 , making it the third most abundant molecule after gaseous H_2 and CO.

Other weaker features at L-band include the 3.54 μm CH_3OH ice band, the 3.47 μm feature likely due to ammonia-water hydrates, the 3.3 μm PAH feature, and potentially the 4.1 μm HDO band. In the M-band, a weak feature around 4.62 μm assigned to OCN^- within the ice is sometimes seen. In the remainder of this article, we discuss a few of the scientific highlights of our programme. More details can be found in the papers by the authors: several of them have been published, whereas others are still in preparation. The reduced spectra will be made available in due course through the Web site <http://www.strw.leidenuniv.nl/~vlchem>

Figure 6: VLT-ISAAC L- and M-band spectra toward the intermediate mass YSO IRAS 08448-4343 in Vela. The spectra are on an optical depth scale and are superposed on a NTT-SOFI H-Ks band image provided by L. Testi.



CO ICE STRUCTURE

One of the major advantages of our sample is the unprecedented combination of high S/N, high spectral resolution, and the large number of sources studied. Indeed, these data show that the solid CO profile is intrinsically very narrow ($\sim 3 \text{ cm}^{-1}$ or $0.007 \mu\text{m}$) and was often not fully resolved in previous observations. Thus, similarities and differences in the profiles for different lines-of-sight can be systematically studied for the first time (Pontopidan et al. 2003a). In earlier analyses, often a ‘mix-and-match’ procedure was followed to fit profiles for individual sources with a variety of laboratory ice mixtures, often leading to degenerate results. Surprisingly, it is found that excellent fits to *all* our spectra can be obtained using a phenomenological decomposition into just three components (Fig. 7). The relative strengths of these components vary from source to source, but their positions and widths are fixed. Only three linear parameters are thus required to fit all CO ice bands ever observed.

This leads to the important conclusion that the CO ice has the same fundamental structure along all lines of sight and that there are at most three different environments for CO on, or in, the ice. Previously, the number of sites was thought to be much larger depending on whether the CO molecule is surrounded by H_2O , CO_2 , CH_3OH , O_2 , CO itself, or any other molecule. Using a simple physical model, it can be shown that for the majority of the lines of sight, 60–90% of the CO ice is in a nearly pure form. This result has sig-

nificant consequences for our understanding of the formation and structure of interstellar ice mantles: either the segregation of the CO and other species has occurred prior or during freeze-out, or subsequent processing of the ice and selective desorption and recondensation have resulted in separation of the components. Figure 7 includes one possible scenario based on recent laboratory experiments where CO is deposited on top of a porous H_2O ice and gradually diffuses into the pores upon heating. If this picture

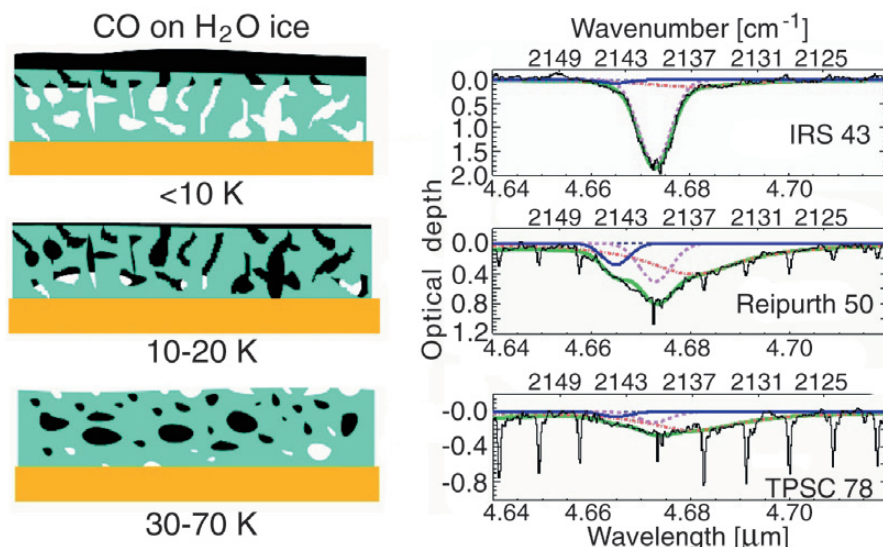


Figure 7: Right: VLT-ISAAC M-band spectra of three sources, showing the decomposition of the solid CO profile into three basic components (blue, purple and orange curves). The green curves indicate the sum of the three components. Left: Sketch of the adsorption, diffusion and desorption behaviour of CO (black) on a porous amorphous H_2O ice (green) as a function of temperature derived from laboratory simulations under pseudo interstellar conditions (Collings et al. 2003, *ApJ* 583, 1058). A one-to-one correspondence of each of these situations with the astronomical spectra can be made.

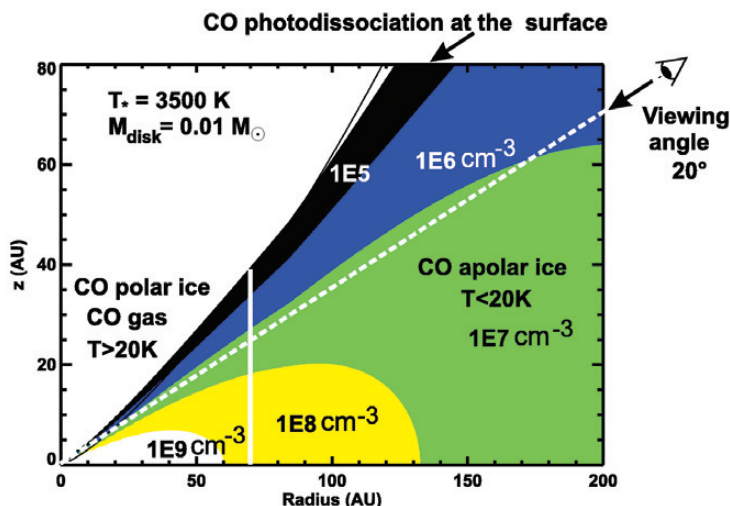
is correct, the shape of the CO profiles can be used as a temperature indicator.

In some sources, the ^{12}CO ice feature is so strong that its isotopic counterparts can be searched for. In our sample, ^{13}CO ice has been seen toward IRS 51 in Ophiuchus, the first detection toward a low-mass YSO. Since ^{13}CO is only a minor component of the ice, its line shape does not depend on the grain shape and allows further constraints to be placed on the CO ice environment. Its profile is indeed consistent with pure CO ice. Finally, a new weak feature at 2175 cm^{-1} ($4.61 \mu\text{m}$) is found in several sources, distinctly offset from the OCN^- band at 2165 cm^{-1} ($4.62 \mu\text{m}$). Since its strength correlates with that of one of the CO components, it is natural to ascribe it to solid CO as well. A feasible match with CO directly bound to the silicate surface has been found in laboratory experiments.

ABUNDANT SOLID CO IN DISCS

A few of our targets are edge-on discs, for which near-infrared images show nebulosities separated by a dark lane. For inclinations of $\sim 10\text{--}20^\circ$, the young star is not completely obscured and the line of sight intercepts a significant fraction of the disc (Fig. 8). One such object is CRBR 2422.8-3423, discovered with VLT imaging. This spectrum shows the deepest solid CO absorption observed to date (Fig. 9) (Thi et al. 2002). Absorption by foreground cloud material likely accounts for only a small fraction of the total solid CO. Gas-phase ro-vibrational CO absorption lines are also detected with a mean temperature of

Figure 8: Sketch of a flaring disc, with different temperature and density zones indicated. The line of sight for the case of CRBR 2422.8–3423 is indicated. CO ice can exist in water-rich ('polar') and water-poor ('apolar') environments depending on temperature.



50 ± 10 K and an average gas/solid CO ratio of ~1 along the line of sight. Such temperatures and ratios are consistent with the flaring disc model sketched in Fig. 8.

Another example is L1489 (Fig. 4), which has a much larger 2000 AU radius disc and is in a transitional state to the T Tauri phase. The high resolution Keck spectra show red-shifted wings on the gaseous CO absorption lines, indicative of infalling motions down to the 0.1 AU scale (Boogert et al. 2002). This illustrates the power of high spectral resolution data to obtain additional kinematic information.

STRONG GASEOUS CO EMISSION: PROBING THE ACCRETION SHOCK?

Many M-band spectra reveal gas-phase CO absorptions in addition to CO ice. A few sources, however, unexpectedly show CO lines in emission (see Fig. 3 and 4). In some cases, these lines are narrow, in other cases they are broad, fully resolved and

have a double-peak structure characteristic of rotation in a disc. A spectacular example is provided by the embedded source GSS30 IRS1 in Ophiuchus, where even emission from ¹³CO and from higher excited ¹²CO levels is detected (Fig. 10) (Pontoppidan et al. 2002). Analysis of the lines shows that the emission originates in a reservoir with 10–100 M_{Earth} of thermalized gas at a well-determined single temperature of ~515 K. Although not conclusive, evidence suggests that the gas is associated with an accretion shock in the disc at 10–100 AU distance, rather than with an outflow.

ABUNDANT CH₃OH: KEY INGREDIENT FOR BUILDING COMPLEX MOLECULES

Another highlight of our program is the first detection of solid methanol towards solar-mass YSO's, thought to be a necessary ingredient for making even larger or-

ganic molecules. Gas-phase species like dimethyl-ether (CH₃OCH₃) and methylformate (CH₃OCHO) have been known in massive YSO's for decades, but their high abundances have been a puzzle to astrochemists, since traditional low-temperature ion-molecule chemistry falls short by orders of magnitude. The currently favored explanation is that evaporation of methanol-rich ices can trigger a high-temperature gas-phase chemistry which can produce complex organic species with abundances close to those observed.

One of the easiest transitions of solid CH₃OH to observe from the ground is at 3.54 μm, superposed on the wing of the water ice band (Fig. 11). Up to now, this feature has only been seen along lines of sight toward high-mass YSO's, but our large programme, together with some follow-up observations, shows detection in at least five low-mass objects, four of them in a small cluster in Serpens (Pontoppidan et al. 2003b). The inferred abundances are as high as 25% of H₂O ice, comparable to the highest solid CH₃OH abundances found toward high-mass YSO's. For other sources, the CH₃OH limits are less than a few % of H₂O ice, consistent with previous limits. This large variation in the solid CH₃OH abundance is not yet understood.

THE ELUSIVE AMMONIA ICE

Another key molecule to identify in the ice is ammonia, NH₃, which is thought to be one of the main nitrogen carriers. Its presence has important consequences, since NH₃ is a strong base and can produce ions through acid-base chemistry, potentially explaining the presence of OCN⁻. Also, experiments in our laborato-

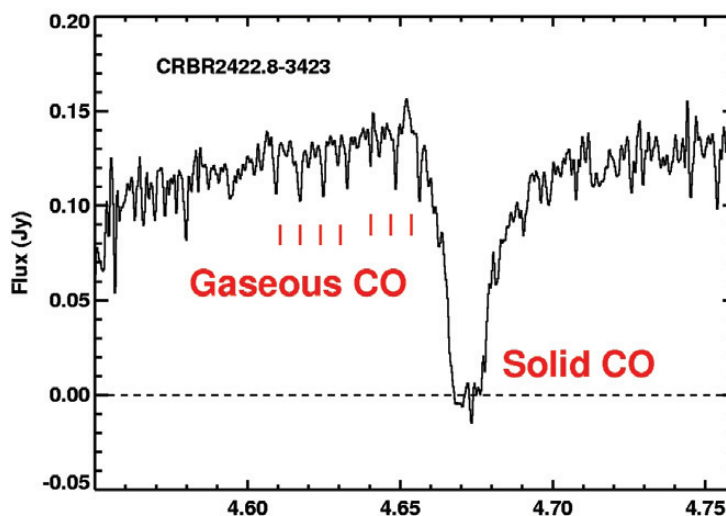
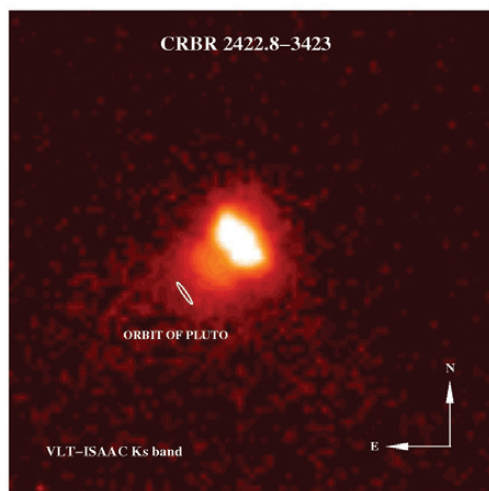


Figure 9: Detection of strong solid CO absorption in the edge-on protoplanetary disk around the solar-mass young star CRBR 2422.8–3423, providing direct evidence for significant freeze-out of CO in the cold layers of the disk. The amount of solid CO is comparable to that of gaseous CO. The VLT-ISAAC Ks archival image of the source shows the dark lane due to the disk crossing the nebula.

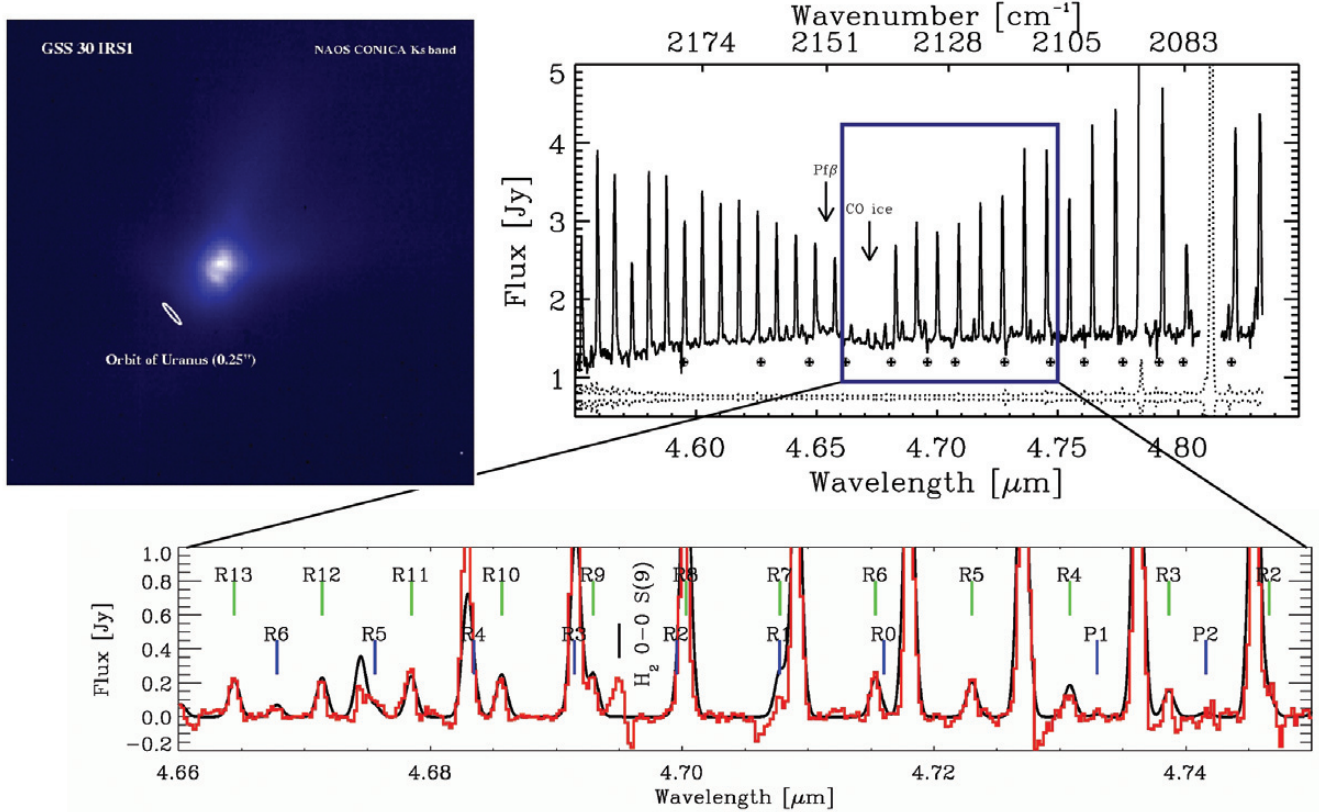


Figure 10: Strong gas-phase CO emission lines found toward the embedded YSO GSS30 originating in ~ 500 K gas within 100 AU from the source. Scattering in the surrounding reflection nebula boosts the strength of the lines. A NAOS-CONICA K-band image, taken in one of our follow-up programmes, is shown as well.

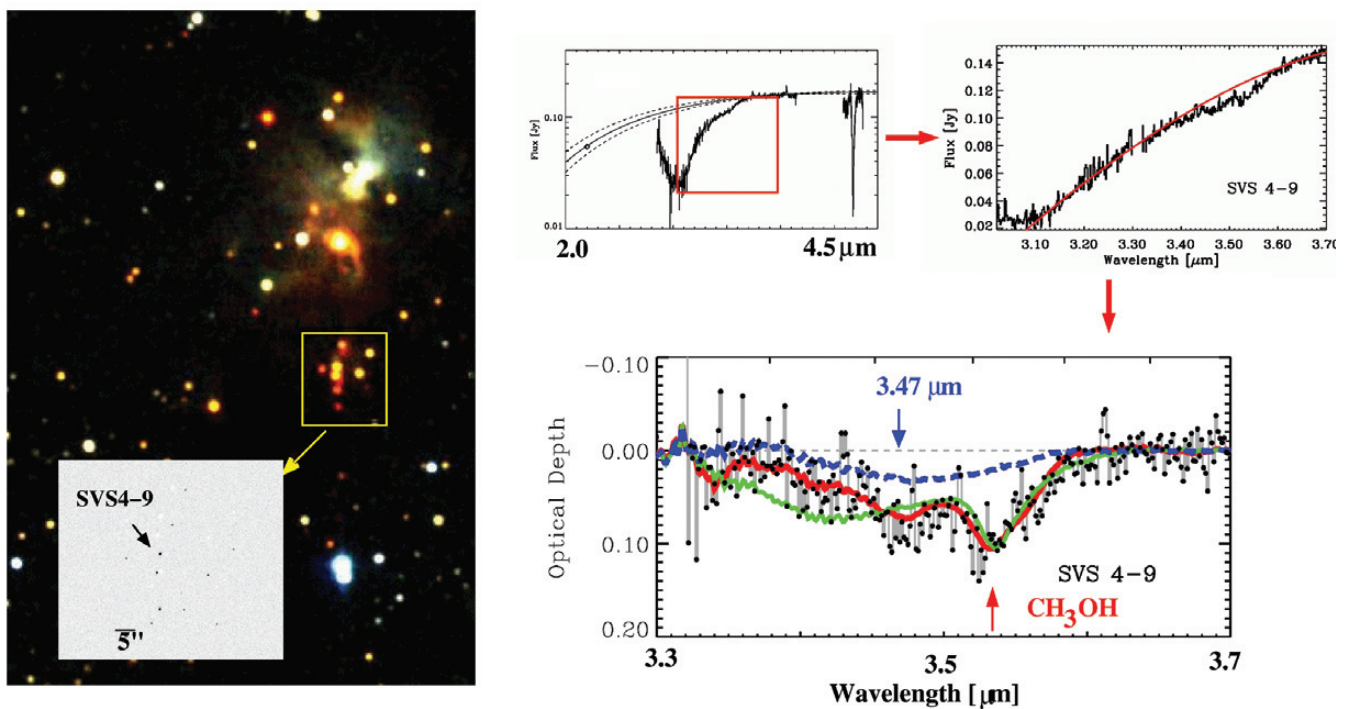


Figure 11: Right: VLT-ISAAC L-band spectra of SVS 4-9 in Serpens, showing the detection of solid CH_3OH in the wing of the solid H_2O band. The $3.47 \mu\text{m}$ feature is also seen. The red and green lines indicate laboratory spectra of solid CH_3OH , either in pure form or mixed with H_2O . Left: 2MASS infrared image of the Serpens core (color), with the VLT acquisition image of the small cluster indicated. Note the excellent VLT image quality ($0.25''$ seeing) resolving the cluster.

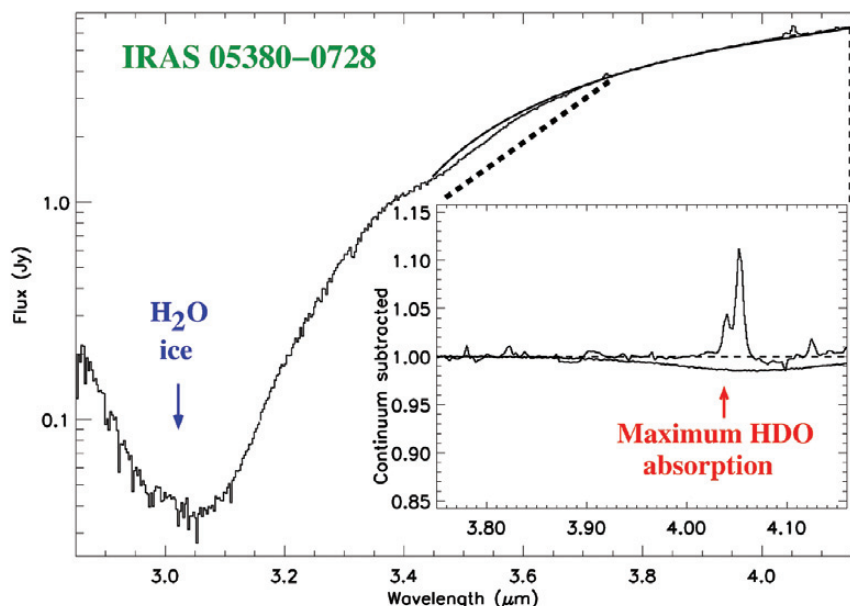


Figure 12: L-band spectrum of IRAS 05380-0728 in Orion, showing the absence of any HDO ice feature at 4.07 μm .

ries and at NASA-Ames have shown that energetic processing of ices containing NH_3 gives rise to complex organic molecules, some of which could be of pre-biological significance, e.g. amino acids. Unfortunately, all of the strong bands of NH_3 overlap with very deep absorptions by H_2O , silicate and other species. A weak NH_3 signature can be obtained from a feature at 3.47 μm , ascribed on the basis of laboratory experiments to a $\text{NH}_3\text{-H}_2\text{O}$ hydrate. This 3.47 μm band is detected in a large fraction of our sources (see Fig. 11 for example) and indicates an amount of NH_3 ice equal to or less than 7% of H_2O ice (Dartois et al. 2002).

Another weak, overtone band of NH_3 occurs at 2.21 μm . Although our heavily obscured sources have very low fluxes in the K-band, we attempted one deep spectrum on the massive YSO W 33A. Earlier analyses of the 9 μm band had inferred a NH_3 abundance of 15% for this source, but our K-band spectrum gives an upper limit of only 5%. This shows the importance of observing more than one band to firmly identify minor species in ices.

HEAVY WATER ICE: LINK WITH COMETS?

Deuterated molecules have long fascinated astrochemists because of the enormous fractionation observed in cold clouds, where the D/H ratios in molecules can be as large as 0.1, more than four orders of magnitude above the overall [D]/[H] abundance ratio of $\sim 1.6 \times 10^{-5}$. Two main explanations have been put forward for these large enhancements: (i) low-temperature gas-phase chemistry, aided by significant CO freeze-out; and

(ii) gas-grain interactions. Detection of deuterated molecules in ice mantles could distinguish between these two scenarios. Heavy water, HDO ice, is the obvious candidate to observe because most of the ice consists of water. It has a feature at 4.07 μm , just at the edge of the atmospheric L-band. As Fig. 12 shows, the feature is not detected, giving typical upper limits $\text{HDO}/\text{H}_2\text{O}$ ice $< 0.002\text{--}0.01$ in various sources (Dartois et al. 2003). These limits are lower than those of gas-phase molecules such as DCN/HCN or HDCO/ H_2CO , but are consistent with the $\text{HDO}/\text{H}_2\text{O}$ ratios of $\sim 3 \cdot 10^{-4}$ found in comets. This favors a scenario in which water is indeed formed on grains and is directly incorporated into (proto-)planetesimals, without participating in the low-temperature gas-phase chemistry.

OUTLOOK

Our large programme summarized here illustrates the power of the VLT and other 8-10 m class telescopes in two areas. First, it has enabled us to obtain high spectral resolution, high quality data on a much larger sample of objects than previously accessible. Second, deeper integrations on selected objects and specific settings have been used to search for minor species or to observe weaker sources. Indeed, weak extragalactic sources are now also within reach and recent VLT-ISAAC M-band spectra of NGC 4945 by Spoon et al. (2003) show very similar features as those found in our sources. Together with the modern surface science, solid-state and gas-phase techniques studied in our laboratories, we have begun to address several puzzles in astrochemistry. Without

access to laboratory work and associated theory, however, these beautiful spectra would constitute an impressive technological accomplishment, but would shed little light on our basic understanding of the physical and chemical processes during star- and planet formation.

Our data base of 3–5 μm spectra will form a valuable reference for future observations of southern YSO's. Many of our sources are part of the SIRTf Legacy 'Cores to Disks' programme (Evans et al. 2003), for which complementary IRS 10–38 μm spectra will be obtained in the coming year. VISIR will be well suited to look for various weak ice bands at longer wavelengths in the same sample, e.g. CH_4 at 7.7 μm and CH_3OH at 9.7 μm . For the gas-phase molecules, the highest spectral resolution modes of VISIR and CRIRES will allow searches for molecules other than CO, both in absorption and emission, opening up new regimes of chemical studies. CRIRES also has the necessary spectral resolution to trace the kinematics.

As emphasized in the introduction, infrared and submillimeter data go hand-in-hand in unravelling the structure of the envelopes and discs around low-mass YSO's. We can hardly wait for ALMA to come on-line and start mapping the millimeter molecular lines in these objects at subarcsec resolution!

ACKNOWLEDGMENTS

We are grateful to the builders of ISAAC for providing such a fine instrument, and to the ESO staff in Garching and at Paranal, in particular F. Comerón, C. Lidman and O. Marco, for their expert support of our programme. We also thank S. Bisschop, I. Taban and W. Alsindi for important contributions.

REFERENCES

- Boogert, A. C. A., Hogerheijde, M. R., & Blake, G. A. 2002, *ApJ* 568, 761
- Dartois, E., Thi, W.-F., Geballe, T. R., et al. 2003, *A&A* 399, 1099
- Dartois, E., d'Hendecourt, L., Thi, W.-F. et al. 2002, *A&A* 394, 1057
- Evans, N. J., Allen, L. E., Blake, G. A. et al. 2003, *PASP* 115, 965
- Spoon, H. W. W., Moorwood, A. F. M., Pontoppidan, K. M., et al. 2003, *A&A* 402, 499
- Pontoppidan, K. M., Fraser, H. J., Dartois, E., et al. 2003a, *A&A*, in press
- Pontoppidan, K. M., Dartois, E., van Dishoeck, E. F., et al. 2003b, *A&A* 404, L17
- Pontoppidan, K. M., Schöier, F. L., van Dishoeck, E. F., & Dartois, E. 2002, *A&A* 393, 585
- Thi, W. F., Pontoppidan, K. M., van Dishoeck, E. F., et al. 2002, *A&A* 394, L27
- van Dishoeck, E. F. & Tielens, A. G. G. M. 2001, in *The Century of Space Science*, eds. J. Bleeker et al. (Kluwer: Dordrecht), p. 607